Augmented PEEC for direct time-domain thermal and power estimation of Integrated Voltage Regulator architectures arising in Heterogeneous Integration

Venkatesh Avula*, Vanessa Smet†, Yogendra Joshi† and Madhavan Swaminathan*
*School of Electrical and Computer Engineering
†George W. Woodruff School of Mechanical Engineering
Georgia Institute of Technology
Atlanta, GA 30332, USA
Email: vavula6@gatech.edu

***Abstract*—An enhanced PEEC model for periodic steady-state analysis is presented. It interprets a dynamical domain as a network of linear and switching elements and represents them with their augmented spectral equivalents. Its computational efficiency is verified on the thermal and power delivery analysis of integrated voltage regulator architectures.**

***Keywords*—Partial Element Equivalent Circuit (PEEC), time-periodic steady-state analysis, heterogeneous integration**

I. Introduction

Heterogeneous integration has become an avenue to reach beyond-Moore's law performance. But the performance comes at a cost of multi-physics challenges. Integrated voltage regulator (IVR), for example, has disparate components like embedded passives and fast-switching GaN devices [1] in close proximity. In implementing such a functionally dense architecture, its multi-physics time-domain characterization is necessary. For example, steady-state temperature response [2] under periodic power cycle loading condition indicates how long the architecture can be run continuously at its peak performance before being overheated and subsequently thermal gated [2]. Similarly, voltage droop response [3] of a power delivery network (PDN) under a switching circuit's step load current determines the power integrity of the system-on-chip (SOC). But in obtaining such time-domain responses, traditional transient time-domain methods are prone to long computation time, instability [4], and integration errors [5].

To circumvent such limitations, an enhanced PEEC model capable of periodic steady-state time-domain analysis is presented in this paper. It combines the PEEC method [5] with the augmented spectral equivalent circuit technique [6]. The augmented PEEC method is particularly advantageous for the aforementioned power and thermal computational problems. For the dynamical thermal domain, it directly solves the steady-state temperature response, while the traditional transient methods suffer from long computation time due to their time-stepping nature and large thermal time-constant of the domain. On the other hand, for the dynamic power delivery analysis, the augmented PEEC method can model the PDN end-to-end as a single black-box, including its DC voltage source, passive interconnects and load switching circuits of SOC, and directly solve the voltage droop response in a single-step, while the traditional methods need separate black-box models, S-parameter model for the interconnects and piece-wise linear (PWL) model for the load switching circuits. Also, the augmented PEEC model is stable, as the model's system stiffness matrix is sparse, full rank and guaranteed to have an inverse due to the Toeplitz nature of its building blocks.

This work was supported in part by ASCENT, one of six centers in JUMP, a Semiconductor Research Corporation (SRC) program sponsored by DARPA.

II. Formulation

Extending the traditional PEEC method's linear time-invariant (LTI) circuit interpretation, the augmented PEEC method considers a given dynamical computational domain as a periodic switched linear (PSL) system. Such a system can be characterized by a Fourier series [7] based bi-frequency transfer function [8]. So we use the Fourier series based augmented spectral equivalent [6] representation for each partial element/variable of the computational domain, assemble the global stiffness matrix from the mesh data of the computational problem, and solve it to determine the unknown periodic steady-state responses of the domain. For the dynamical power and thermal domains considered in this paper, their equivalent PSL systems are DC or '0' frequency excited, which simplifies their augmented representations. Note that the simplified framework given below is analogous to and extends [9] the harmonic balance method for the class of PSL systems.

A. Augmented PEEC computational framework

The augmented framework uses a complex exponential basis set. For a dynamical computational domain or PSL system, the switching frequency of its switch or time-varying source, ω_s, is used as the fundamental frequency of the basis.

978-1-7281-6161-7/20/$31.00 ©2020 IEEE

Authorized licensed use limited to: Georgia Institute of Technology. Downloaded on December 08,2020 at 15:03:17 UTC from IEEE Xplore. Restrictions apply.

The number of positive harmonics of the fundamental, N, determine the fidelity of the steady-state response. For a time-varying variable or switching element of the PSL system, the coefficients of the basis are the Fourier coefficients of its respective time-varying characteristic. The basis expansion for such a variable and switch is given in eqs. 1 and 2 respectively.

$$X(t) = \sum_{n=-N}^{+N} X_n e^{-jn\omega_s t} \tag{1}$$

where $X(t) \in \mathbb{R}$ and $X_n \in \mathbb{C}$ are its Fourier coefficients.

$$Y_{sw}(t) = \sum_{n=-N}^{+N} Y_n e^{-jn\omega_s t} \tag{2}$$

where $Y_{sw}(t) \in \mathbb{R}$ is the switch's time-varying periodic conductance profile, and $Y_n \in \mathbb{C}$ are its Fourier coefficients.

Based on the basis above, the augmented spectral equivalents for the variables, elements and excitation sources of a dynamical domain are listed in Table I. Classic LTI elements-resistors, conductance, capacitors and inductors- become diagonal matrices, while time-varying switches become Toeplitz matrices. Similarly, the time-varying variables and sources of the domain, like voltages and currents, become vectors.

TABLE I
AUGMENTED BLACKBOX REPRESENTATIONS [a]

Element/variable	Augmented spectral equivalent representation
Laplace, s	$\tilde{s} = j\omega_s.diag(\left[-N, \ldots, 0, \ldots, N\right]) \in \mathbb{R}^{D\times D}$
Voltage, V	$\tilde{V} = \left[V_{-N}, \ldots, V_0, \ldots, V_N\right]^T \in \mathbb{R}^{D\times 1}$
Temperature, T	$\tilde{T} = \left[T_{-N}, \ldots, T_0, \ldots, T_N\right]^T \in \mathbb{R}^{D\times 1}$
Current, I	$\tilde{I} = \left[I_{-N}, \ldots, I_0, \ldots, I_N\right]^T \in \mathbb{R}^{D\times 1}$
Heat flux, Q_{sw}	$\tilde{Q}_{sw} = \left[Q_{-N}, \ldots, Q_0, \ldots, Q_N\right]^T \in \mathbb{R}^{D\times 1}$
DC source, E_{DC}	$\tilde{E}_{DC} = \left[0, \ldots, E_{DC}, \ldots, 0\right]^T \in \mathbb{R}^{D\times 1}$
Scalar, k	$\tilde{k} = k.diag(\left[1, \ldots, 1, \ldots, 1\right]) \in \mathbb{R}^{D\times D}$
Resistor, R	$\tilde{R} = R.diag(\left[1, \ldots, 1, \ldots, 1\right]) \in \mathbb{R}^{D\times D}$
Inductor, L	$\tilde{L} = L.diag(\left[1, \ldots, 1, \ldots, 1\right]) \in \mathbb{R}^{D\times D}$
Capacitor, C	$\tilde{C} = C.diag(\left[1, \ldots, 1, \ldots, 1\right]) \in \mathbb{R}^{D\times D}$
Conductance, G	$\tilde{G} = G.diag(\left[1, \ldots, 1, \ldots, 1\right]) \in \mathbb{R}^{D\times D}$
Switch 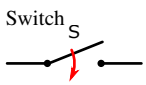	$\tilde{Y}_{sw} = \begin{bmatrix} Y_0 & Y_{-1} & \ldots & Y_{-2N} \\ Y_1 & Y_0 & \ldots & Y_{-2N+1} \\ \vdots & \vdots & \ddots & \vdots \\ Y_{2N} & Y_{2N-1} & \ldots & Y_0 \end{bmatrix}_{D\times D}$

[a] augmented basis dimension, $D = 2N + 1$ for N positive harmonics

B. Augmented Thermal PEEC

Representing the finite-difference method's (FDM) [10] thermal cells using the augmented matrix forms from Table I and applying Kirchhoff's current law (KCL), the following augmented circuit eq. 3 can be written.

$$\left[\tilde{s}\tilde{C} + \tilde{G}\right]\left[\tilde{T}\right] = \left[\tilde{Q}_{sw}\right] \tag{3}$$

where $\tilde{Q}_{sw}$ is the time-varying heat flux load. $\tilde{C}$ and $\tilde{G}$ are the augmented capacitance and conductance.

The solved nodal temperature, $\tilde{T}$, of eq. 3 can then be converted to time-domain profiles, T(t), using eq. 1.

C. Augmented PDN PEEC

The dynamical PDN can be modeled as an equivalent circuit consisting of RLCG elements [11], DC source and a switching load. Using the augmented matrix representation from Table I and applying KCL and Kirchhoff's voltage law (KVL), the following augmented circuit eq. 4 can be written.

$$\begin{bmatrix} \tilde{s}\tilde{C} + \tilde{G} + \tilde{Y}_{sw} & \tilde{A} \\ \tilde{A}^T & -(\tilde{R} + \tilde{s}\tilde{L}) \end{bmatrix} \begin{bmatrix} \tilde{V} \\ \tilde{I} \end{bmatrix} = \begin{bmatrix} \tilde{I}_S = \vec{0} \\ \tilde{E}_{DC} \end{bmatrix} \tag{4}$$

where $\tilde{A}$ is augmented incidence matrix, $\tilde{Y}_{sw}$ is switching load device, $\tilde{I}_S$ is current source, a null vector for our case, $\tilde{E}_{DC}$ is DC excitation voltage source and $\tilde{I}$ is unknown current profile.

The solved nodal voltage, $\tilde{V}$, of eq. 4 can then be converted to time-domain voltage droop profile, V(t), using eq. 1.

III. RESULTS

IVR architectures, shown in Fig. 1, are used as test cases to validate the proposed method and evaluate their performance. For thermal validation, a 500 quad element 2D mesh of the 2D IVR case is run in both the Wolfram Mathematica FEM package having 561 nodal unknowns and the proposed augmented PEEC method having 500×21 or 10500 unknowns with the boundary and loading conditions shown in Figs.1a and 2a. Similarly, for the power domain, 3D IVR package PDN is modeled with Ansys HFSS and is run in Keysight ADS based transient under the 1A current step loading and equivalent circuit conditions shown in Figs. 3a and 3b. 3D IVR's PDN include via and c4 arrays, while the 2d IVR additionally include parallel planes. SOC die is modeled as C_{die} of 50nF with parasitic resistances of 2mΩ. The validation study results are shown in Figs. 2b, 3c, and Table II, while the evaluation study results are in Figs. 2c, 3d and Table III.

IV. DISCUSSION

The validation results, in Figs. 2b and 3c, show perfect match and thus validate the proposed method. Table II shows that it is 2500x faster. On the other hand, typical PDN's time constant is much smaller, so its steady-state response is identical to the transient right from the start, as shown in Fig. 3c. So the method addresses the time-scale challenges in multi-physics. Also, multiple tools like ADS and HFSS were needed to generate the transient, while the augmented PEEC did it seamlessly in a single-step. Multi-physics evaluation results in Table III show that the 3D IVR performs better in power delivery but is thermally-limited. Short and direct current path, as highlighted in Fig. 1b, results in lower voltage droop for the 3D IVR, while the lateral power planes in the 2D IVR, as in Fig. 1a, cause additional loop inductance, resulting in its higher voltage droop. Also, comparing temperature maps, in Figs. 2d and 2e, indicate that the 3D IVR's embedded inductors are in the hotspot, therefore needing advanced thermal management solutions. As part of future work, Numerical inverse Laplace transform (NILT) [9] technique can be explored to capture the initial transient response from 0 to 20s in Fig. 2b. Joule heating caused by electro-thermal coupling can also be explored for a more accurate temperature profile.

Authorized licensed use limited to: Georgia Institute of Technology. Downloaded on December 08,2020 at 15:03:17 UTC from IEEE Xplore. Restrictions apply.

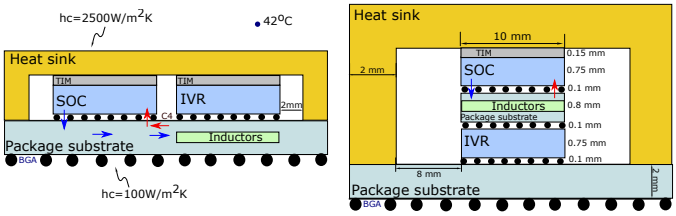

(a) 2D IVR architecture (b) 3D IVR architecture

Fig. 1. Heterogeneously integrated voltage regulator (IVR) architectures

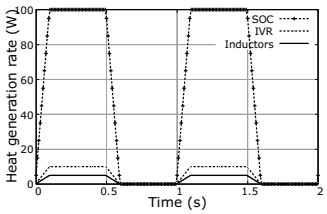

(a) Periodic heat flux loading profiles with time period, T_s=1s

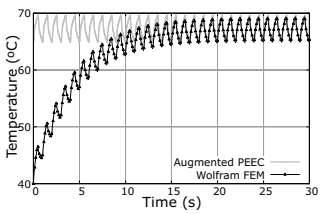

(b) Inductor's response for the 2D IVR case: comparison with reference

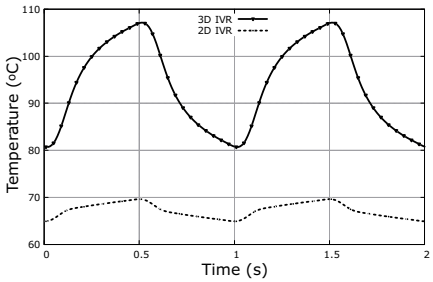

(c) Inductor's response: 2D vs. 3D IVR

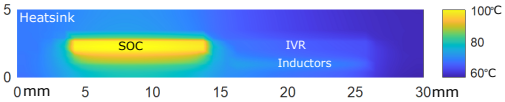

(d) Temperature map of 2D IVR at 0.5s

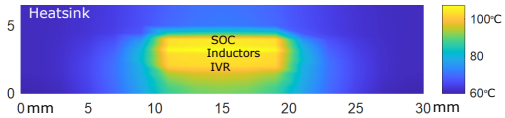

(e) Temperature map of 3D IVR at 0.5s

Fig. 2. Augmented PEEC based thermal analysis

TABLE II
STEADY-STATE RESPONSE COMPUTATION TIME COMPARISON[a]

Test case	Wolfram FEM	Augmented PEEC with N=10
2D IVR	173s	0.07s

[a]run on Intel Core i7 system with 16GB RAM.

TABLE III
IVR ARCHITECTURE EVALUATION USING THE AUGMENTED PEEC [a]

Test case	Voltage droop (mV)	$T_{inductor}$(°C)
2D IVR	22	70
3D IVR	3.25	107

[a]with number of positive harmonics, N=10 for thermal and 20 for PDN.

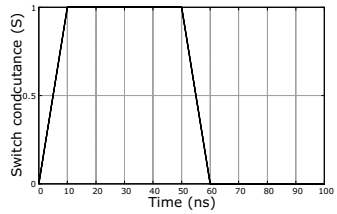

(a) SOC's switching load profile

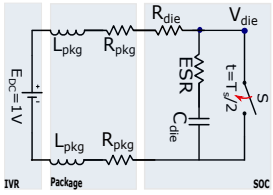

(b) Equivalent circuit representation of the dynamical PDN

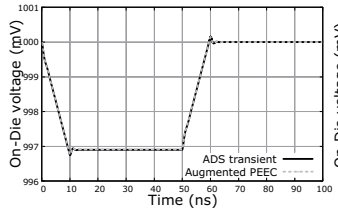

(c) Droop response for the 3D IVR case: comparison with reference

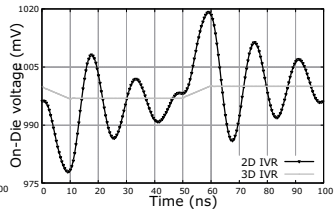

(d) Droop response: 2D vs. 3D IVR

Fig. 3. Augmented PEEC based power delivery analysis

V. CONCLUSION

An extended PEEC model capable of direct time-periodic steady-state analysis is presented. From the test cases involving power and thermal evaluation of heterogeneously integrated voltage regulators, this paper shows that the proposed method is seamless and agile for dynamic multi-physics modeling.

REFERENCES

[1] V. Avula and S. Sandler, "Evaluation of Gallium Nitride HEMTs for VRM designs," presented at the DesignCon, 2016.

[2] S. K. Khatamifard, L. Wang, W. Yu, S. Köse, and U. R. Karpuzcu, "Thermogater: Thermally-aware on-chip voltage regulation," in *2017 ACM/IEEE 44th Annual International Symposium on Computer Architecture (ISCA)*, 2017, pp. 120–132.

[3] K. Aygün, M. J. Hill, K. Eilert, K. Radhakrishnan, and A. Levin, "Power delivery for high-performance microprocessors." *Intel Technology Journal*, vol. 9, no. 4, pp. 273 – 283, 2005.

[4] V. Avula and A. Zadehgol, "A novel method for equivalent circuit synthesis from frequency response of multi-port networks," in *2016 International Symposium on Electromagnetic Compatibility - EMC EUROPE*, 2016, pp. 79–84.

[5] A. Ruehli, "Partial element equivalent circuit (PEEC) method and its application in the frequency and time domain," in *Proceedings of Symposium on Electromagnetic Compatibility*, 1996, pp. 128–133.

[6] R. Trinchero, I. S. Stievano, and F. G. Canavero, "Steady-state analysis of switching power converters via augmented time-invariant equivalents," *IEEE Transactions on Power Electronics*, vol. 29, no. 11, pp. 5657–5661, 2014.

[7] T. Strom and S. Signell, "Analysis of periodically switched linear circuits," *IEEE Transactions on Circuits and Systems*, vol. 24, no. 10, pp. 531–541, 1977.

[8] L. A. Zadeh, "Frequency analysis of variable networks," *Proceedings of the IRE*, vol. 38, no. 3, pp. 291–299, March 1950.

[9] R. Trinchero, I. S. Stievano, and F. G. Canavero, "Simulation of buck converters via numerical inverse Laplace transform," in *2017 IEEE 21st Workshop on Signal and Power Integrity (SPI)*, 2017, pp. 1–4.

[10] L. Lombardi, R. Raimondo, and G. Antonini, "Electrothermal formulation of the partial element equivalent circuit method," *International Journal of Numerical Modelling: Electronic Networks, Devices and Fields*, vol. 31, no. 4, p. e2253, 2018, e2253 jnm.2253.

[11] Y. Li *et al.*, "Analysis of multilayer structure near- and far-field radiation by the coupled PP-PEEC and field-equivalence principle method," *IEEE Transactions on Electromagnetic Compatibility*, vol. 61, no. 2, pp. 495–503, 2019.

Authorized licensed use limited to: Georgia Institute of Technology. Downloaded on December 08,2020 at 15:03:17 UTC from IEEE Xplore. Restrictions apply.